

in the SAXS-WAXS instrument of the Dubble beamline BM26 at the ESRF. The length of the SAXS instrument was chosen such that the long spacing reflection of CB was detected within the SAXS signal. We followed the process at different temperatures until almost all CB was solidified.

In this abstract we concentrate on just one typical example, where the molten CB is cooled to 20° C. After 6 minutes the long spacing shows up at d-value 67.4 Å and in the next half hour this value slowly decreases to 64.75 Å where it stays. From these values we conclude that the crystallisation starts from SOA and successively SOS, POS and POP are taking part. The intensity indicates that after an hour almost all CB has been crystallised. The CB crystallites are very small; at the initial stages they are 35 nm, which doubles in an hour to 67 nm. In matured chocolate the sizes may be up to 250 nm. So even then an average crystal consists of 40 layers, or 20 times the crystallographic c-axis.

The crystallisation process is preceded by a broad WAXS signal around a 80-85 Å, which fades away when the long spacing shows up. This signal most probably corresponds to a triple layer with a very unordered oleic middle region. At present this is studied in more detail.

In the presentation other time-resolved experiments will be shown as well.

[1] J.B. van Mechelen, R. Peschar, H. Schenk, *Acta Cryst.* **2006**, B62, 1121-1130. [2] J.B. van Mechelen, R. Peschar, H. Schenk, *Acta Cryst.* **2006**, B62, 1131-1138.

Keywords: nano-crystals in cocoa butter, time-resolved XRPD, SAXS-WAXS

MS74.P13

Acta Cryst. (2011) A67, C675

Crystal Structure of Monoclinic $\text{Sr}_{2.4}\text{Ca}_{0.6}\text{Al}_2\text{O}_6$

James A. Kaduk,^a Winnie Wong-Ng,^b Joseph T. Golab,^c ^a*Illinois Institute of Technology, Chicago IL 60616 (USA)*. ^b*NIST, Gaithersburg MD 20899 (USA)*. ^c*Ineos Technologies, Naperville IL 60563 (USA)*. E-mail: kaduk@polycrystallography.com

Although the Portland cement related phases $\text{Sr}_x\text{Ca}_{3-x}\text{Al}_2\text{O}_6$ have been reported to crystallize in the cubic space group *Pa3* for the whole solid solution range, a monoclinic form of $\text{Sr}_{2.4}\text{Ca}_{0.6}\text{Al}_2\text{O}_6$ was prepared at 1300EC. Indexing the powder pattern was challenging; the strong split peaks could be indexing on a small orthorhombic cell, and the supercell tools in the old program NBS*LATTICE were used to identify a 32H monoclinic supercell which accounted for all of the peaks. The space group was identified as *P2₁/c* by examining possible distortions of the *Pa3* structure using ISODISTORT. $\text{Sr}_{2.4}\text{Ca}_{0.6}\text{Al}_2\text{O}_6$ crystallizes in *P2₁/c*, with $a = 15.7244(8)$, $b = 15.7361(2)$, $c = 15.7265(8)$ Å, $\beta = 90.6235(11)^\circ$, and $V = 3891.13(28)$ Å³. The lowering of the symmetry results in the presence of two independent 6-rings of corner-sharing AlO_4 tetrahedra; one 6-ring is more distorted than the other. The Sr/Ca are mostly ordered; at only one of the 20 alkaline earth sites is the occupation ~50/50. The Ca are not clustered in the unit cell. Symmetry mode analysis shows that the distortion from the cubic structure is complex, but concentrated in oxygen displacements in a few modes. The as-prepared sample contains some amorphous material, which hydrates to $\text{Sr}_3\text{Al}_2(\text{OH})_{12}$ on storage. Even in a combined synchrotron/laboratory Rietveld refinement (with extensive use of bonded and non-bonded distance restraints) it was difficult to obtain a precise structure. The final coordinates were determined by a density functional geometry optimization using the fixed experimental unit cell.

Keywords: strontium, aluminate, rietveld

MS74.P14

Acta Cryst. (2011) A67, C675

Grafting lactic acid on calcium-zinc hydroxyapatite surface

Debbabi Mongi, Turki Thouraya, Aissa Abdallah, *Laboratoire de Physico-Chimie des Matériaux, Faculté des Sciences de Monastir, 5019 Monastir (Tunisie)*. E-mail: m.debbabi@yahoo.fr

Solid solutions of calcium-zinc hydroxyapatite $[\text{Ca}_{10-x}\text{Zn}_x(\text{PO}_4)_6(\text{OH})_2]$ with $0 \leq x \leq 2$, were synthesized by a wet process in a basic medium [1]. The surface modification was carried out by dissolution of lactic acid in the organic suspension of hydroxyapatite. The hybrid organic-inorganic derivatives are characterized by means of element analysis, X-ray powder diffraction, infrared and NMR-MAS ¹³C spectroscopies. Chemical analyses indicate that the grafting process was ameliorated by the increase of the acid concentration and/or the zinc content. The X-ray powder diffraction patterns shows the conservation of apatitic structure as a unique crystalline phase with a low affectation of cristallinity which increases with increasing of acid concentration in solution. This affectation is more remarkable for phases richest in zinc. Other than characteristic bands of phosphate [ν_s (961 cm⁻¹), δ_s (474 cm⁻¹), ν_{as} (1032 cm⁻¹), δ_{as} (564 cm⁻¹)] and hydroxyl groups [ν_s (3570 cm⁻¹), ν_L (630 cm⁻¹)] of hydroxyapatite, infrared spectra display news vibration modes related to lactic acid essentially in the range from 1400 to 1600 cm⁻¹. The NMR-MAS ¹³C spectra of hydroxyapatite treated present three peaks centered around 20, 69 and 182 ppm which are attributed to the three carbons of lactic acid. The signal at 182 ppm characterizing the quaternary carbon ($\text{C}=\text{O}$) was degenerated on two or three signals respectively for hydroxyapatite containing one or two zinc atoms. This can be due to the heterogeneity of carbon environment by the presence of zinc at the apatitic surface.

[1] T. Turki, A. Aissa, H. Agougui, M. Debbabi, *Journal de la Société Chimique de Tunisie*, **2010**, 12, 161-172.

Keywords: apatite, diffraction, spectroscopy.

MS74.P15

Acta Cryst. (2011) A67, C675-C676

Fonctionnalisation of calcium-zinc hydroxyapatite by tartaric acid

Turki Thouraya, Aissa Abdallah, Debbabi Mongi, *Laboratoire de Physico-Chimie des Matériaux, Faculté des Sciences de Monastir, Avenue de l'environnement 5019 Monastir (Tunisie)*. E-mail: tourkithouraya@yahoo.fr

Solid solutions of calcium-zinc hydroxyapatite $[\text{Ca}_{10-x}\text{Zn}_x(\text{PO}_4)_6(\text{OH})_2]$ with $0 \leq x \leq 2$, were synthesized by a wet process in a basic medium [1]. The functionalization of their surface was carried out by dissolution of tartaric acid in organic suspension. The news hybrid inorganic-organic composites, $\text{Ca}_{10-x}\text{Zn}_x(\text{PO}_4)_6(\text{OH})_2$ -Tartaric acid obtained are characterized by means of elemental analysis, X-ray powder diffraction, FT-IR and NMR-MAS ¹³C spectroscopies. Chemical analyses approve the functionalization of hydroxyapatite and indicate that grafting process was ameliorated by the increasing of acid concentration and/or the zinc content. The X-ray powder diffraction patterns shows the conservation of apatitic structure as unique crystalline phase. The cristallinity was affected slightly as function of acid concentration increases in start solution. This affectation is more remarkable for phases richest in zinc. The relative FT-IR absorption spectra display the absorption bands characteristic of PO_4^{3-} modes [ν_s (961 cm⁻¹), δ_s (474 cm⁻¹), ν_{as} (1032 cm⁻¹), δ_{as} (564 cm⁻¹)], and the absorption bands [ν_s (3570 cm⁻¹), ν_L (630 cm⁻¹)] due to the stretching and libration modes of OH⁻ groups. In addition, news absorption bands

appear at 1416 and 1609 cm^{-1} characteristic respectively to symmetric and anti-symmetric vibration of COO^- of tartaric acid. The intensity of COO^- bands increases as function of acid concentration in solution and with zinc content, implying the formation of calcium and zinc tartarate on the hydroxyapatite surface. The NMR-MAS ^{13}C spectra of hydroxyapatite treated present two peaks at 74 and 181 ppm characteristic of two different carbons of tartaric acid. The formation of new hybrid compounds was confirmed by the shift of signals comparing with those of free tartaric acid. Moreover, the broadening of these peaks can be explained by the heterogeneity of carbon environment by the presence of zinc on the apatitic surface.

[1] T. Turki, A. Aissa, H. Agougui, M. Debbabi, *journal de la société chimique de tunisie*, **2010**, 12, 161-172.

Keywords: apatite, surface, fonctionnel

MS74.P16

Acta Cryst. (2011) A67, C676

How to deal with multiple solutions in powder pattern indexing

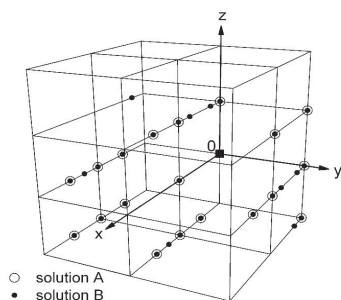
Rolf Heinemann, Diedrich Stöckelmann and Herbert Kroll, *Institut für Mineralogie, WWU Münster (Germany)*. E-mail: rhein_03@uni-muenster.de

Santoro et al (1980) [1] first addressed the question of equivalence when in powder pattern indexing more than one indexing solution and thus more than one reciprocal metric tensor are produced. Two metric tensors G_A^* and G_B^* are said to be equivalent when a matrix R exists such that $G_B^* = R G_A^* R^T$ (1). R is a 3×3 non-symmetric matrix consisting of rational numbers. Therefore, eq. (1) cannot be solved directly. Santoro et al (1980) [1] suggested to vary the elements of R systematically in the range (5, -5) until the equality sign in eq. (1) is fulfilled within chosen error limits.

We suggest a different procedure: First, the three shortest non-coplanar vectors that have the same Q values in both lattices A and B are identified. These vectors are taken to define a new basis common to A and B . Then, 3×3 matrices M_A and M_B are written which transform the axial systems of A and B into the new one. If the new axial system reproduces lattices A and B , then the equality $M_A G_A^* M_A^T = M_B G_B^* M_B^T$ (2) holds. Eq. (2) defines a new metric tensor common to both lattices A and B which we thus term the common metric tensor G_C^* . The coordinates of the reciprocal lattice points of A and B are transformed according to $(\eta/\kappa/\lambda)_{A,B} = (M_{A,B}^{-1})^T (h/k/l)_{A,B}$. Coincident lattice points yield $(\eta/\kappa/\lambda)_A = (\eta/\kappa/\lambda)_B$. If all lattice points coincide, lattices A and B are termed equivalent; if only a subset of points is coincident, the lattices are semi-equivalent; otherwise they are non-equivalent.

Equation (1) can be easily retrieved from equation (2): $G_B^* = M_B^{-1} M_A G_A^* M_A^T (M_B^{-1})^T = R G_A^* R^T$. Thereby we arrive at a solution to eq. (1) that avoids trial and error methods.

We take as an example two different indexing solutions A and B to $\text{CrPO}_4 \cdot 6\text{H}_2\text{O}$, given by Santoro et al. (1980) [1], to demonstrate the spatial relationship of the respective reciprocal lattice points. Fig. 1 shows that lattice points A and B coincide. However, solution A only explains a subset of points.



○ solution A
● solution B

[1] A. Santoro, A.D. Mighell, J.R. Rodgers, *Acta Cryst.* **1980**, A36, 796-800.

Keywords: powder pattern indexing, multiple solutions, metric tensor

MS74.P17

Acta Cryst. (2011) A67, C676

XRD and SAXS studies applied to doped Polyaniline and Poly(*o*-methoxyaniline)

Edgar Ap. Sanches,^a Juliana C. Soares,^a Graziella Trovati,^b Yvonne P. Mascarenhas,^a ^aUniversity of São Paulo (USP), Institute of Physics of São Carlos (IFSC), (Brazil). ^bUniversity of São Paulo (USP), Institute of Chemistry of São Carlos (IQSC), (Brazil). E-mail: edgar.sanches@ifsc.usp.br

Polyaniline (PANI) and derivatives of aniline have received great attention due to their technological applications. The introduction of polar functional groups and alkyl groups to the main chain of PANI is a practice to obtain soluble polymers in a wider variety of organic solvents. Poly(*o*-methoxyaniline) (POMA) is a derivative of PANI and its structural difference is the presence of the group ($-\text{OCH}_3$) in the *ortho* position of the carbon rings, been extensively studied in the form of powder or films for the most various applications. ES-PANI and ES-POMA were synthesized, respectively, according to the method described elsewhere [1,2] with times of synthesis ranging from 0,5 to 96 h. Samples were characterized by XRD, SAXS, LeBail Fit [3], SEM and van der Pauw method [4]. XRD analysis showed that the synthesis time was not significant in the crystallinity of PANI, however, it is an important parameter in the synthesis of POMA, which became more crystalline. LeBail Fit showed that the ES-PANI crystallites average size is 34 Å, while for ES-POMA the crystallites average size increases with increasing synthesis time (from 26 to 57 Å). By SAXS it was possible to obtain values of Radius of Giration (R_g) (217 Å for ES-PANI and 280 – 313 Å for ES-POMA); the maximum particle size (D_{max}) from the Pair-distance distribution Function ($p(r)$) (650 Å for ES-PANI and 900 Å for ES-POMA) and the particle organization qualitative analysis through Kratky curves, showing that for ES-PANI the crystallinity does not increase significantly over synthesis; for ES-POMA, particles became more ordered with increasing of crystallinity over the synthesis. Images of SEM allowed the visualization of different morphologies for PANI and POMA: while the PANI-ES showed fiber morphology formed by interconnected nanospheres, the POMA-ES had a globular vesicular morphology, which changed with increasing synthesis time. Conductivity measurements were not changed drastically in different synthesis time for ES-PANI ($1,84 \cdot 10^{-4} \text{S/cm}$), whereas for the ES-POMA the conductivity increased during the synthesis ($1,89 \cdot 10^{-7}$ to $8,89 \cdot 10^{-7} \text{S/cm}$). The results obtained by each of the techniques were essential to the understanding of the structure and properties of polymeric materials.

[1] S. Bhadra, N.K. Singha, D. Khastgir. *Journal of Applied Polymer Science* **2007**, 104, 1900–1904. [2] J.M. Yeh, C.P. Chin. *Journal of Applied Polymer Science* **2003**, 88, 1072–1080. [3] A. LeBail, H. Duroy, J.L. Fourquet. *Materials Research Bulletin* **1988**, 23, 447–452. [4] R. Robert, S.M. Berleze, *Revista Brasileira de Ensino de Física* **2007**, 29, 15-18.

Keywords: polyaniline, poly(*o*-methoxyaniline), XRD

MS74.P18

Acta Cryst. (2011) A67, C676-C677

The magnetic ordering in Mn_3TeO_6 and Co_3TeO_6

Roland Tellgren,^a Sergey Ivanov,^{ab} Per Nordblad,^b Roland Mathieu,^b